
Batch Normalization Biases Residual Blocks Towards the Identity Function in Deep Networks

Soham De
DeepMind, London
sohamde@google.com

Samuel L. Smith
DeepMind, London
sllsmith@google.com

Abstract

Batch normalization dramatically increases the largest trainable depth of residual networks, and this benefit has been crucial to the empirical success of deep residual networks on a wide range of benchmarks. We show that this key benefit arises because, at initialization, batch normalization downscals the residual branch relative to the skip connection, by a normalizing factor on the order of the square root of the network depth. This ensures that, early in training, the function computed by normalized residual blocks in deep networks is close to the identity function (on average). We use this insight to develop a simple initialization scheme that can train deep residual networks without normalization. We also provide a detailed empirical study of residual networks, which clarifies that, although batch normalized networks can be trained with larger learning rates, this effect is only beneficial in specific compute regimes, and has minimal benefits when the batch size is small.

1 Introduction

The combination of skip connections [1–3] and batch normalization [4] dramatically increases the largest trainable depth of neural networks. Although the origin of this effect is poorly understood, it has led to a rapid improvement in the performance of deep networks on popular benchmarks [5, 6]. Following the introduction of layer normalization [7] and the transformer architecture [8, 9], almost all state-of-the-art networks currently contain both skip connections and normalization layers.

Our contributions. This paper provides a simple explanation for why batch normalized deep residual networks are trainable. We prove that batch normalization downscals the hidden activations on the residual branch by a factor on the order of the square root of the network depth (at initialization). Therefore, as the depth of a residual network is increased, the residual blocks are increasingly dominated by the skip connection, which drives the functions computed by residual blocks closer to the identity, preserving signal propagation and ensuring well-behaved gradients [10–14].

If our theory is correct, it should be possible to train deep residual networks without normalization, simply by downscaling the residual branch. Therefore, to verify our analysis, we introduce a one-line code change (“SkipInit”) which imposes this property at initialization, and we confirm that this alternative scheme can train one thousand layer residual networks without normalization.

In addition, we provide a detailed empirical study of residual networks at a wide range of batch sizes. This study demonstrates that, although batch normalization does enable us to train residual networks with larger learning rates, we only benefit from using large learning rates in practice if the batch size is large. When the batch size is small, normalized and unnormalized networks have similar optimal learning rates, yet normalized networks still achieve significantly higher test accuracies and lower training losses. These experiments confirm that large learning rates are not the primary benefit of batch normalization in residual networks, contrary to the claims made by previous work [15, 16].

Paper layout. In section 2, we prove that residual blocks containing identity skip connections and normalization layers are biased towards the identity function in deep networks (at initialization). To confirm that this property explains why deep normalized residual networks are trainable, we propose a simple alternative to normalization (“SkipInit”) that shares the same property at initialization, and we provide an empirical study of normalized residual networks and SkipInit at a range of network depths. In section 3, we study the performance of residual networks at a range of batch sizes, in order to clarify when normalized networks benefit from large learning rates. We study the regularization benefits of batch normalization in section 4 and we compare the performance of batch normalization, SkipInit and Fixup [17] on ImageNet in section 5. We discuss related work in section 6.

2 Why are deep normalized residual networks trainable?

2.1 Theoretical analysis at initialization

Residual networks (ResNets) [2, 3] contain a sequence of residual blocks, which are composed of a “residual branch” comprising a number of convolutions, normalization layers and non-linearities, as well as a “skip connection”, which is usually just the identity (See figure 1). While introducing skip connections shortens the effective depth of the network, on their own they only increase the trainable depth by roughly a factor of two [18]. Normalized residual networks, on the other hand, can be trained for depths significantly deeper than twice the depth of their non-residual counterparts [3, 17].

To understand this effect, we analyze the variance of hidden activations at initialization. For clarity, we focus here on the variance of a single training example, but we discuss the variance across batches of training examples (which share the same random weights) in appendix C. Let x_i^ℓ denote the i -th component of the input to the ℓ -th residual block, where x_i^1 denotes the input to the model with $\mathbf{E}(x_i^1) = 0$ and $\mathbf{Var}(x_i^1) = 1$ for each independent component i . Let f^ℓ denote the function computed by the residual branch of the ℓ -th residual block, $x_i^+ = \max(x_i, 0)$ denote the output of the ReLU, and \mathcal{B} denote the batch normalization operation (for completeness, we define batch normalization formally in appendix A). For simplicity, we assume that there is a single linear layer on each residual branch, such that for normalized networks, $f^\ell(x^\ell) = W^\ell \mathcal{B}(x^\ell)^+$, and for unnormalized networks $f^\ell(x^\ell) = W^\ell x^\ell^+$. We also assume that each component of W^ℓ is independently sampled from $\mathcal{N}(0, 2/\text{fan-in})$ (He Initialization) [19].¹ Thus, given x^ℓ , the mean of the i -th coordinate of the output of a residual branch $\mathbf{E}(f_i^\ell(x^\ell)|x^\ell) = 0$. Since $x^{i+1} = x^i + f^\ell(x^i)$, this implies $\mathbf{E}(x_i^\ell) = 0$ for all ℓ . The covariance between the residual branch and the skip connection $\mathbf{Cov}(f_i^\ell(x^\ell), x_i^\ell) = 0$, and therefore the variance of the hidden activations, $\mathbf{Var}(x_i^{\ell+1}) = \mathbf{Var}(x_i^\ell) + \mathbf{Var}(f_i^\ell(x^\ell))$. We conclude:

Unnormalized networks: If the residual branch is unnormalized, the variance of the residual branch, $\mathbf{Var}(f_i^\ell(x^\ell)) = \sum_j^{\text{fan-in}} \mathbf{Var}(W_{ij}^\ell) \cdot \mathbf{E}((x_j^{\ell+1})^2) = 2 \cdot \mathbf{E}((x_i^{\ell+1})^2) = \mathbf{Var}(x_i^\ell)$. This has two implications. First, the variance of the hidden activations explode exponentially with depth, $\mathbf{Var}(x_i^{\ell+1}) = 2 \cdot \mathbf{Var}(x_i^\ell) = 2^\ell$. One can prevent this explosion by introducing a factor of $(1/\sqrt{2})$ at the end of each residual block, such that $x^{i+1} = (x^i + f^\ell(x^i))/\sqrt{2}$. Second, since $\mathbf{Var}(f_i^\ell(x^\ell)) = \mathbf{Var}(x_i^\ell)$, the residual branch and the skip connection contribute equally to the output of the residual block. This ensures that the function computed by the residual block is far from the identity function.

Normalized networks: If the residual branch is normalized, the variance of the output of the residual branch $\mathbf{Var}(f_i^\ell(x^\ell)) = \sum_j^{\text{fan-in}} \mathbf{Var}(W_{ij}^\ell) \cdot \mathbf{E}((\mathcal{B}(x_j^\ell)^2) = \mathbf{Var}(\mathcal{B}(x^\ell)) \approx 1$.² Thus, the variance of the input to the ℓ -th residual block, $\mathbf{Var}(x_i^\ell) \approx \mathbf{Var}(x_i^{\ell-1}) + 1$, which implies $\mathbf{Var}(x_i^\ell) \approx \ell$. Surprisingly, the growth in the variance of the hidden activations is beneficial, because if $\mathbf{Var}(x_i^\ell) \approx \ell$,

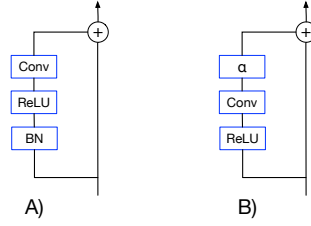


Figure 1: A) A residual block with batch normalization. It is common practice to include two convolutions on the residual branch; we show one convolution for simplicity. B) SkipInit replaces batch normalization by a single learnable scalar α . We set $\alpha = 0$ (or a small constant) at initialization.

¹fan-in denotes the number of incoming network connections to the layer.

²The approximation is tight when the batch size for computing the batch statistics is large.

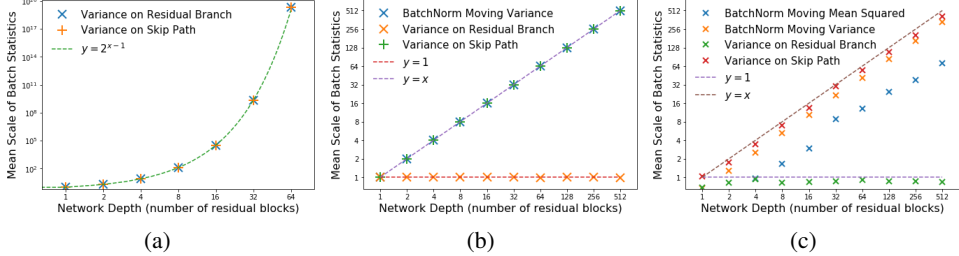


Figure 2: We empirically evaluate the dependence of the variance of the hidden activations on the depth of the residual block at initialization (See appendix B for details). In (a), we consider a fully connected ResNet with linear activations without any normalization, evaluated on random Gaussian inputs. In (b), we consider the same ResNet but with one normalization layer on each residual branch. The squared BatchNorm moving mean is close to zero (not shown). In (c), we consider a batch normalized convolutional residual network with ReLU activations, evaluated on CIFAR-10.

then the batch normalization operation \mathcal{B} must suppress the variance of the ℓ -th residual branch by a factor of ℓ (hidden activations are suppressed by $\sqrt{\ell}$). Consequently, the residual branch contributes only a $1/(\ell + 1)$ fraction of the variance in the output of the ℓ -th residual block. This ensures that, at initialization, the outputs of most residual blocks in a deep normalized ResNet are dominated by the skip connections, which biases the function computed by the residual block towards the identity. The depth of a typical residual block is on the order of the total number of residual blocks d , which implies that batch normalization downscale residual branches by a factor on the order of \sqrt{d} . Although this is weaker than the factor of d proposed in the initialization study of [12], we find empirically in section 2.3 that it is sufficiently strong to train deep residual networks with 1000 layers.

To verify our analysis, we evaluate the variance of the hidden activations, as well as the batch normalization statistics, of three residual networks at initialization in figure 2. We define the networks in appendix B. In figure 2(a), we consider a fully connected linear unnormalized residual network, where we find that the variance on the skip path of the ℓ -th residual block matches the variance of the residual branch and is equal to $2^{\ell-1}$, as predicted by our analysis. In figure 2(b), we consider a fully connected linear normalized residual network, where we find that the variance on the skip path of the ℓ -th residual block is approximately equal to ℓ , while the variance at the end of each residual branch is approximately 1. The batch normalization moving variance on the ℓ -th residual block is also approximately equal to ℓ , confirming that batch normalization downscale the residual branch by a factor of $\sqrt{\ell}$ as predicted. In figure 2(c), we consider a normalized convolutional residual network with ReLU activations evaluated on CIFAR-10. The variance on the skip path remains proportional to the depth of the residual block, with a coefficient slightly below 1 (likely due to zero padding at the image boundary). The batch normalization moving variance is also proportional to depth, but slightly smaller than the variance across channels on the skip path. We show in appendix C that this occurs because ReLU activations introduce correlations between different examples in the mini-batch. These correlations also cause the square of the batch normalization moving mean to grow with depth.

2.2 SkipInit; an initialization scheme to verify our analysis

We claim above that batch normalization enables us to train deep residual networks, because (in expectation) it downscale the residual branch at initialization by a normalizing factor on the order of the square root of the network depth. To provide further evidence for this claim, we now propose a simple initialization scheme that can train deep residual networks without normalization, ‘‘SkipInit’’:

SkipInit: Include a scalar multiplier at the end of each residual branch, initialized to α .

After normalization is removed, it should be possible to implement SkipInit as a one line code change. In section 2.3, we show that we can train deep residual networks, so long as α is initialized at a value of $(1/\sqrt{d})$ or smaller, where d denotes the total number of residual blocks (see table 1). Notice that this observation agrees exactly with our analysis of deep normalized residual networks in section 2.1. In practice, we recommend setting $\alpha = 0$, so that the residual block represents the identity function at initialization. This choice is also simpler to apply, since it ensures the initialization scheme is independent of network depth. We note that SkipInit is designed for residual networks that contain an identity skip connection such as the ResNet-V2 [3] or Wide-ResNet architectures [20]. We discuss how to extend SkipInit to the original ResNet-V1 [2] formulation of residual networks in appendix F.

Table 1: Batch normalization enables us to train deep residual networks. We can recover this benefit without normalization if we introduce a scalar multiplier α on the end of the residual branch and initialize $\alpha = (1/\sqrt{d})$ or smaller (where d is the number of residual blocks). In practice, we advocate initializing $\alpha = 0$. We provide optimal test accuracies and optimal learning rates with error bars.

Batch Normalization			SkipInit ($\alpha = 1$)		
Depth	Test accuracy	Learning rate	Depth	Test accuracy	Learning rate
16	93.5 ± 0.1	$2^{-1} (2^{-1} \text{ to } 2^{-1})$	16	93.0 ± 0.1	$2^{-2} (2^{-2} \text{ to } 2^{-1})$
100	94.7 ± 0.1	$2^{-1} (2^{-2} \text{ to } 2^{-0})$	100	—	—
1000	94.6 ± 0.1	$2^{-2} (2^{-3} \text{ to } 2^{-0})$	1000	—	—
SkipInit ($\alpha = 1/\sqrt{d}$)			Divide residual block by $\sqrt{2}$		
Depth	Test accuracy	Learning rate	Depth	Test accuracy	Learning rate
16	93.0 ± 0.1	$2^{-2} (2^{-2} \text{ to } 2^{-1})$	16	92.4 ± 0.1	$2^{-2} (2^{-2} \text{ to } 2^{-1})$
100	94.2 ± 0.1	$2^{-1} (2^{-2} \text{ to } 2^{-1})$	100	88.9 ± 0.4	$2^{-5} (2^{-5} \text{ to } 2^{-5})$
1000	94.2 ± 0.0	$2^{-1} (2^{-2} \text{ to } 2^{-1})$	1000	—	—
SkipInit ($\alpha = 0$)			SkipInit without L2 ($\alpha = 0$)		
Depth	Test accuracy	Learning rate	Depth	Test accuracy	Learning rate
16	93.3 ± 0.1	$2^{-2} (2^{-2} \text{ to } 2^{-2})$	16	89.8 ± 0.2	$2^{-3} (2^{-3} \text{ to } 2^{-3})$
100	94.2 ± 0.1	$2^{-2} (2^{-2} \text{ to } 2^{-2})$	100	91.7 ± 0.2	$2^{-2} (2^{-2} \text{ to } 2^{-2})$
1000	94.3 ± 0.2	$2^{-2} (2^{-3} \text{ to } 2^{-1})$	1000	92.1 ± 0.1	$2^{-2} (2^{-2} \text{ to } 2^{-2})$

2.3 An empirical study of residual networks at a wide range of network depths

We empirically verify the claims made above by studying the minimal components required to train deep residual networks. In table 1, we report the mean test accuracy of an n -2 Wide-ResNet [20], trained on CIFAR-10 for 200 epochs at batch size 64 at a range of depths n between 16 and 1000 layers. At each depth, we train the network 7 times for a range of learning rates on a logarithmic grid, and we measure the mean and standard deviation of the test accuracy for the best 5 runs (this procedure ensures that our results are not corrupted by outliers or failed runs). The optimal test accuracy is the mean performance at the learning rate whose mean test accuracy was highest, and we always verify that the optimal learning rates are not at the boundary of our grid search. Here and throughout this paper, we use SGD with heavy ball momentum, and fix the momentum coefficient $m = 0.9$. Although we tune the learning rate on the test set, we emphasize that our goal is not to achieve state of the art results. Our goal is to compare the performance of different training procedures, and we apply the same experimental protocol in each case. We hold the learning rate constant for 100 epochs, before dropping the learning rate by a factor of 2 every 10 epochs. This simple schedule achieves higher test accuracies than the original 3 drops schedule proposed in [2]. We apply data augmentation including per-image standardization, padding, random crops and left-right flips. We use L2 regularization with a coefficient of 5×10^{-4} , and we initialize convolutional layers using He initialization [19]. We provide the corresponding optimal training losses in appendix D.

As expected, batch normalized Wide-ResNets are trainable for a wide range of depths, and the optimal learning rate is only weakly dependent on the depth. We can recover this effect without normalization by incorporating SkipInit and initializing $\alpha = (1/\sqrt{d})$ or smaller, where d denotes the number of residual blocks. This provides strong evidence to support our claim that batch normalization enables us to train deep residual networks by biasing residual blocks towards the skip path at initialization. Just like normalized networks, the optimal learning rate with SkipInit is almost independent of the network depth. SkipInit slightly underperforms batch normalization on the test set at all depths, although we show in appendix D that it achieves similar training losses to normalized networks.

For completeness, we verify that one cannot train deep residual networks with SkipInit if $\alpha = 1$. We also confirm that for unnormalized residual networks, it is not sufficient merely to ensure the activations do not explode on the forward pass (which can be achieved by multiplying the output of each residual block by $(1/\sqrt{2})$). Note that we do not provide results in table 1 in cases where the test accuracy was frozen at random initialization throughout training at all learning rates. Finally, we noticed that, at initialization, the loss in deep networks is dominated by the L2 regularization term, causing the weights to shrink rapidly early in training. To clarify whether this effect is necessary, we evaluated SkipInit ($\alpha = 0$) without L2 regularization. We find that L2 regularization is not necessary for trainability. This demonstrates that we can train deep residual networks without normalization and without reducing the scale of the weights at initialization, solely by downscaling the hidden activations on the residual branch. We provide additional results on CIFAR-100 in appendix E.

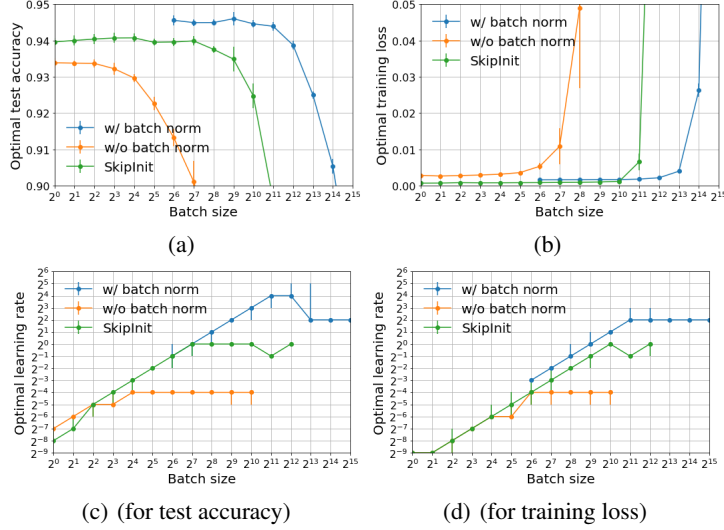


Figure 3: In (a), we achieve higher test accuracy with batch normalization than without batch normalization, and we are also able to train efficiently at much larger batch sizes. SkipInit substantially reduces the gap in performance for small/moderate batch sizes, but it still underperforms batch normalization when the batch size is large. In (b), SkipInit achieves smaller training losses than batch normalization for batch sizes $b \lesssim 1024$. We provide the test accuracy at the learning rate for which the test accuracy was maximized, and the training loss at the learning rate for which the training loss was minimized. To help interpret these results, we also provide the optimal learning rates in figures (c) and (d). All three methods have similar optimal learning rates when the batch size is small, but batch normalization and SkipInit are able to scale to larger learning rates when the batch size is large.

3 When can normalized networks benefit from large learning rates?

In two widely read papers, Santurkar et al. [15] and Bjorck et al. [16] argued that the primary benefit of batch normalization is that it improves the conditioning of the loss landscape, which allows us to train with larger learning rates. However, this claim seems incompatible with a number of recent papers studying optimization in deep learning [21–26]. These papers argue that if we train for a fixed number of epochs (as is common in practice), then when the batch size is small, the optimal learning rate is also small, since it is constrained by the noise in the gradient estimate. In this small batch regime, the optimal learning rate is usually proportional to the batch size [27, 28]. Meanwhile the conditioning of the loss sets the maximum stable learning rate [25, 26, 29], and this controls how large we can make the batch size before the performance of the model begins to degrade. If this perspective is correct, we would expect large learning rates to be beneficial only when the batch size is also large. In this section, we clarify the role of large learning rates in normalized networks by studying residual networks with and without batch normalization at a wide range of batch sizes.

In figure 3, we provide results of a 16-4 Wide-ResNet, trained on CIFAR-10 for 200 epochs at a wide range of batch sizes and learning rates. We follow the same experimental protocol described in section 2.3, however we average over the best 12 out of 15 runs. To enable us to consider extremely large batch sizes on a single GPU, we evaluate the batch statistics over a “ghost batch size” of 64, before accumulating gradients to form larger batches, as is standard practice [30]. We therefore are unable to consider batch sizes below 64 with batch normalization. Note that we repeat this experiment in the small batch limit in section 4, where we evaluate the batch statistics over the full training batch.

Unsurprisingly, the performance with batch normalization is better than the performance without batch normalization on both the test set and the training set at all batch sizes.³ However, both with and without batch normalization, the optimal test accuracy is independent of batch size in the small batch limit, before beginning to decrease when the batch size exceeds some critical threshold.⁴ Crucially,

³Note that we provide the training loss excluding the L2 regularization term. Normalized networks often achieve smaller L2 losses because the network function is independent of the scale of the weights.

⁴As the batch size grows, the number of parameter updates decreases since the number of training epochs is fixed. We note that the performance might not degrade with batch size under a constant step budget [24].

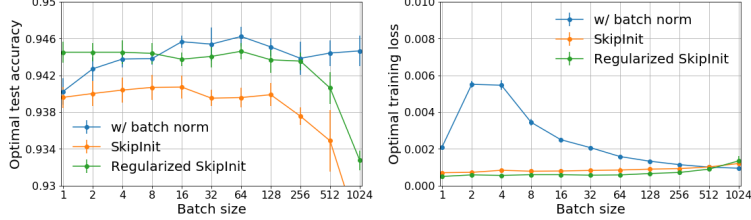


Figure 4: To study the regularization benefits of batch normalization, we evaluate the batch statistics over the full batch, allowing us to consider any batch size $b \geq 1$. The training loss falls as the batch size increases, but the test accuracy is maximized for an intermediate batch size, $b \approx 64$. Regularized SkipInit outperforms batch normalization on the test set for small batch sizes.

this threshold is significantly larger when batch normalization is used, which demonstrates that one can efficiently scale training to larger batch sizes in normalized networks. SkipInit reduces the gap in test accuracy between normalized and unnormalized networks, and it achieves smaller training losses than batch normalization when the batch size is small ($b \lesssim 1024$). However similar to unnormalized networks, it still performs worse than normalized networks when the batch size is very large.

To explain why normalized networks can scale training to larger batch sizes, we provide the optimal learning rates that maximize the test accuracy and minimize the training loss in figures 3(c) and 3(d). When the batch size is small, the optimal learning rates are proportional to the batch size, and the optimal learning rate is similar with and without batch normalization. However when the batch size is large, the optimal learning rates are independent of batch size [25, 26], and normalized networks use larger learning rates. Intuitively, this transition occurs when we reach the maximum stable learning rate, above which training diverges [29]. Our results confirm that batch normalized networks have a larger maximum stable learning rate than SkipInit networks, which have a larger maximum stable learning rate than unnormalized networks. This explains why batch normalized networks were able to efficiently scale training to larger batch sizes. Crucially however, our experiments confirm that batch normalized networks do not benefit from the use of large learning rates when the batch size is small.

Furthermore, under a fixed epoch budget, the highest test accuracies for all three methods are always achieved in the small batch limit with small learning rates, and the test accuracy never increases when the batch size rises. We therefore conclude that large learning rates are not the primary benefit of batch normalization in residual networks, contradicting the claims of earlier work [15, 16]. The primary benefit of batch normalization is that it biases the residual blocks in deep residual networks towards the identity function, thus enabling us to train significantly deeper networks. To emphasize this claim, we show in the next section that the gap in test accuracy between batch normalization and SkipInit in the small batch limit can be further reduced with additional regularization. We provide additional results sweeping the batch size on a 28-10 Wide-ResNet on CIFAR-100 in appendix E.

4 On the regularization benefit of batch normalization

It is widely known that batch normalization can have a regularizing effect [30], and most authors believe that this benefit arises from the noise that occurs when the batch statistics are estimated on a subset of the full training set [31]. In this section, we study this regularization benefit at a range of batch sizes. Unlike the previous section (which used a “ghost batch size” of 64 [30]), in this section we will evaluate the batch statistics of normalized networks over the entire mini-batch. We introduced SkipInit in section 2.2, which ensures that very deep unnormalized ResNets are trainable. To attempt to recover the additional regularization benefits of batch normalization, we now introduce “Regularized SkipInit”. This scheme includes SkipInit ($\alpha = 0$), but also introduces biases to all convolutions and applies a single Dropout layer [32] before the softmax with drop probability 0.6.

In figure 4, we provide the performance of our 16-4 Wide-ResNet at a range of batch sizes in the small batch limit (note that batch normalization reduces to instance normalization when the batch size $b = 1$). We provide the corresponding optimal learning rates in appendix D. The test accuracy of batch normalized networks initially improves as the batch size rises, before decaying for batch sizes $b \gtrsim 64$. Meanwhile, the training loss increases as the batch size rises from 1 to 2, but then decreases consistently as the batch size rises further. This confirms that noise arising from uncertainty in the batch statistics does have a generalization benefit if properly tuned. This is why we chose a ghost batch size of 64 in section 3. The performance of SkipInit and Regularized SkipInit are independent

Table 2: When training ResNet50-V2 on ImageNet, SkipInit and Fixup are competitive with batch normalization for small batch sizes, while batch normalization performs best when the batch size is large. SkipInit and Fixup both achieve higher validation accuracies than batch normalization with extra regularization. We train for 90 epochs and perform a grid search to identify the optimal learning rate which maximizes the top-1 validation accuracy. We perform a single run at each learning rate and report top-1 and top-5 accuracy scores. We use a drop probability of 0.2 when Dropout is used.

Test accuracy:	Batch size		
	256	1024	4096
Batch normalization	75.0 / 92.2	74.9 / 92.1	74.9 / 91.9
Fixup	74.8 / 91.8	74.6 / 91.7	73.0 / 90.6
SkipInit + Biases	74.9 / 91.9	74.6 / 91.8	70.8 / 89.2
Fixup + Dropout	75.8 / 92.5	75.6 / 92.5	74.8 / 91.8
Regularized SkipInit	75.6 / 92.4	75.5 / 92.5	72.7 / 90.7

of batch size in the small batch limit, and Regularized SkipInit achieves higher test accuracies than batch normalization when the batch size is very small. Note that we introduced Dropout [32] to show that extra regularization may be necessary to close the performance gap between normalized and SkipInit networks, but more sophisticated regularizers would likely achieve higher test accuracies. We provide additional results studying this regularization effect on CIFAR-100 in appendix E.

5 A Comparison on ImageNet

In this section, we compare the performance of batch normalization and SkipInit on ImageNet. For completeness, we also compare to the recently proposed Fixup initialization [17]. Since SkipInit is designed for residual networks with an identity skip connection, we consider the ResNet50-V2 architecture [3]. We provide additional experiments on ResNet50-V1 [2] in appendix F. We use the original architectures and match the performance reported by [33] (we do not apply the popular modifications to these architectures described in [21]). We train for 90 epochs, and when batch normalization is used we set the ghost batch size to 256. The learning rate is linearly increased from 0 to the specified value over the first 5 epochs of training [21], and then held constant for 40 epochs, before decaying it by a factor of 2 every 5 epochs. As before, we tune the learning rate at each batch size on a logarithmic grid. We provide the optimal validation accuracies in table 2. We found that adding biases to the convolutional layers led to a small boost in accuracy for SkipInit, and we therefore included biases in all SkipInit runs. SkipInit and Fixup match the performance of batch normalization at the standard batch size of 256, however both SkipInit and Fixup perform worse than batch normalization when the batch size is very large. Both SkipInit and Fixup achieve higher test accuracies than batch normalization with extra regularization (Dropout) for small batch sizes.

6 Related Work

In recent years, almost all state-of-the-art models have involved applying some kind of normalization scheme [4, 7, 34–36] in combination with skip connections [1–3, 8, 9]. Although some authors have succeeded in training very deep networks without normalization layers or skip connections [14, 37], these papers required careful orthogonal initialization schemes that are not compatible with ReLU activation functions. Baldazzi et al. [11] and Yang et al. [13] argued that ResNets with identity skip connections and batch normalization layers on the residual branch preserve correlations between different minibatches in deep networks, and Baldazzi et al. [11] suggested that this effect can be mimicked by initializing deep networks close to linear functions. However, even deep linear networks are difficult to train with Gaussian weights [12, 18, 37], which suggests that imposing linearity at initialization is not sufficient. Veit et al. [10] observed empirically that normalized residual networks are typically dominated by short paths, however they did not identify the cause of this effect. Some authors have studied initialization schemes which multiply the output of the residual branch by a fixed scalar (smaller than 1), without establishing a link to normalization methods [12, 38–41].

Zhang et al. [17] proposed Fixup initialization, and confirmed that it can train both deep residual networks and deep transformers without normalization layers. Fixup contains four components:

1. The classification layer and final convolution of each residual branch are initialized to zero.
2. The initial weights of the remaining convolutions are scaled down by $d^{-1/(2m-2)}$, where d denotes the number of residual branches and m is the number of convolutions per branch.

3. A scalar multiplier is introduced at the end of each residual branch, initialized to one.
4. Scalar biases are introduced before every layer in the network, initialized to zero.

The authors do not relate these components to the influence of the batch normalization layers on the residual branch, or seek to explain why deep normalized ResNets are trainable. They argue that the second component of Fixup is essential, however our experiments in section 2.3 demonstrate that this component is not necessary to train deep residual networks at typical batch sizes. In practice, we have found that either component 1 or component 2 of Fixup on its own is sufficient in ResNet-V2 networks, since both components downscale the hidden activations on the residual branch (fulfilling the same role as SkipInit). We found in section 5 that SkipInit and Fixup have similar performance for small batch sizes but that Fixup slightly outperforms SkipInit when the batch size is large.

7 Discussion

Our work demonstrates that batch normalization has three main benefits. In order of importance,

1. Batch normalization can train deep residual networks (section 2).
2. Batch normalization increases the maximum stable learning rate (section 3).
3. Batch normalization has a regularizing effect (section 4).

This work explains benefit 1, by observing that batch normalization biases residual blocks towards the identity function at initialization. This ensures that deep residual networks have well-behaved gradients, enabling efficient training [10–13, 18]. Note that our argument naturally extends to other normalization variants and model architectures, including layer normalization [7] and “pre-norm” transformers [9] (where the normalization layers are on the residual branch). A single normalization layer per residual branch is sufficient, and normalization layers should not be placed on the skip path (as in the original transformer [8]). We can recover benefit 1 without normalization by introducing a learnable scalar multiplier on the residual branch initialized to zero. This simple change can train deep ResNets without normalization, and often enhances the performance of shallow ResNets.

The conditioning benefit (benefit 2) is not necessary when one trains with small batch sizes, but it remains beneficial when one wishes to train with large batch sizes. Since large batch sizes can be computed in parallel across multiple devices [21], this could make normalization necessary in time-critical situations, for instance if a production model is retrained frequently in response to changing user preferences. Also, since batch normalization has a regularizing effect (benefit 3), it may be necessary in some architectures if one wishes to achieve the highest possible test accuracy. Note however that one can sometimes exceed the test accuracy of normalized networks by introducing alternate regularizers (see section 5 or [17]). We therefore believe future work should focus on identifying an alternative to batch normalization that recovers its conditioning benefits.

We would like to comment briefly on the similarity between SkipInit for residual networks, and Orthogonal initialization of vanilla fully connected tanh networks [37]. Orthogonal initialization is currently the only initialization scheme capable of training deep networks without skip connections. It initializes the weights of each layer as an orthogonal matrix, such that the activations after a linear layer are a rotation (or reflection) of the activations before the layer. Meanwhile, the tanh non-linearity is approximately equal to the identity for small activations over a region of scale 1 around the origin. Intuitively, if the incoming activations are mean centered with scale 1, they will pass through the non-linearity almost unchanged. Since rotations compose, the approximate action of the entire network at initialization is to rotate (or reflect) the input. Like residual blocks with SkipInit, the influence of a fully connected layer with orthogonal weights will therefore be close to the identity in function space. However ReLUs are not compatible with orthogonal initialization, since they are not linear about the origin, which has limited the use of orthogonal initialization in practice.

To conclude. Batch normalization biases the residual blocks of deep residual networks towards the identity function (at initialization). This ensures that the network has well behaved-gradients, and it is therefore a major factor behind the excellent empirical performance of normalized residual networks in practice. We show that one can recover this benefit in unnormalized residual networks with a one line code change to the architecture (“SkipInit”). In addition, we clarify that, although batch normalized networks can be trained with larger learning rates than unnormalized networks, this is only useful for large batch sizes and does not have practical benefits when the batch size is small.

Acknowledgements

We thank Jeff Donahue, Chris Maddison, Erich Elsen, James Martens, Razvan Pascanu, Chongli Qin, Karen Simonyan, Yann Dauphin, Esme Sutherland and Yee Whye Teh for various discussions that have helped improve the paper.

References

- [1] Rupesh Kumar Srivastava, Klaus Greff, and Jürgen Schmidhuber. Highway networks. *arXiv preprint arXiv:1505.00387*, 2015.
- [2] Kaiming He, Xiangyu Zhang, Shaoqing Ren, and Jian Sun. Deep residual learning for image recognition. In *Proceedings of the IEEE conference on computer vision and pattern recognition*, pages 770–778, 2016.
- [3] Kaiming He, Xiangyu Zhang, Shaoqing Ren, and Jian Sun. Identity mappings in deep residual networks. In *European conference on computer vision*, pages 630–645. Springer, 2016.
- [4] Sergey Ioffe and Christian Szegedy. Batch normalization: Accelerating deep network training by reducing internal covariate shift. *arXiv preprint arXiv:1502.03167*, 2015.
- [5] Mingxing Tan and Quoc V Le. Efficientnet: Rethinking model scaling for convolutional neural networks. *arXiv preprint arXiv:1905.11946*, 2019.
- [6] Qizhe Xie, Eduard Hovy, Minh-Thang Luong, and Quoc V Le. Self-training with noisy student improves imagenet classification. *arXiv preprint arXiv:1911.04252*, 2019.
- [7] Jimmy Lei Ba, Jamie Ryan Kiros, and Geoffrey E Hinton. Layer normalization. *arXiv preprint arXiv:1607.06450*, 2016.
- [8] Ashish Vaswani, Noam Shazeer, Niki Parmar, Jakob Uszkoreit, Llion Jones, Aidan N Gomez, Łukasz Kaiser, and Illia Polosukhin. Attention is all you need. In *Advances in neural information processing systems*, pages 5998–6008, 2017.
- [9] Alec Radford, Jeffrey Wu, Rewon Child, David Luan, Dario Amodei, and Ilya Sutskever. Language models are unsupervised multitask learners. *OpenAI Blog*, 1(8):9, 2019.
- [10] Andreas Veit, Michael J Wilber, and Serge Belongie. Residual networks behave like ensembles of relatively shallow networks. In *Advances in neural information processing systems*, pages 550–558, 2016.
- [11] David Balduzzi, Marcus Frean, Lennox Leary, JP Lewis, Kurt Wan-Duo Ma, and Brian McWilliams. The shattered gradients problem: If resnets are the answer, then what is the question? In *Proceedings of the 34th International Conference on Machine Learning-Volume 70*, pages 342–350. JMLR. org, 2017.
- [12] Boris Hanin and David Rolnick. How to start training: The effect of initialization and architecture. In *Advances in Neural Information Processing Systems*, pages 571–581, 2018.
- [13] Greg Yang, Jeffrey Pennington, Vinay Rao, Jascha Sohl-Dickstein, and Samuel S Schoenholz. A mean field theory of batch normalization. *arXiv preprint arXiv:1902.08129*, 2019.
- [14] Lechao Xiao, Yasaman Bahri, Jascha Sohl-Dickstein, Samuel S Schoenholz, and Jeffrey Pennington. Dynamical isometry and a mean field theory of cnns: How to train 10,000-layer vanilla convolutional neural networks. *arXiv preprint arXiv:1806.05393*, 2018.
- [15] Shibani Santurkar, Dimitris Tsipras, Andrew Ilyas, and Aleksander Madry. How does batch normalization help optimization? In *Advances in Neural Information Processing Systems*, pages 2483–2493, 2018.
- [16] Nils Bjorck, Carla P Gomes, Bart Selman, and Kilian Q Weinberger. Understanding batch normalization. In *Advances in Neural Information Processing Systems*, pages 7694–7705, 2018.

- [17] Hongyi Zhang, Yann N Dauphin, and Tengyu Ma. Fixup initialization: Residual learning without normalization. *arXiv preprint arXiv:1901.09321*, 2019.
- [18] Karthik A Sankararaman, Soham De, Zheng Xu, W Ronny Huang, and Tom Goldstein. The impact of neural network overparameterization on gradient confusion and stochastic gradient descent. *arXiv preprint arXiv:1904.06963*, 2019.
- [19] Kaiming He, Xiangyu Zhang, Shaoqing Ren, and Jian Sun. Delving deep into rectifiers: Surpassing human-level performance on imagenet classification. In *Proceedings of the IEEE international conference on computer vision*, pages 1026–1034, 2015.
- [20] Sergey Zagoruyko and Nikos Komodakis. Wide residual networks. *arXiv preprint arXiv:1605.07146*, 2016.
- [21] Priya Goyal, Piotr Dollár, Ross Girshick, Pieter Noordhuis, Lukasz Wesolowski, Aapo Kyrola, Andrew Tulloch, Yangqing Jia, and Kaiming He. Accurate, large minibatch sgd: Training imagenet in 1 hour. *arXiv preprint arXiv:1706.02677*, 2017.
- [22] Samuel L Smith, Pieter-Jan Kindermans, Chris Ying, and Quoc V Le. Don’t decay the learning rate, increase the batch size. *arXiv preprint arXiv:1711.00489*, 2017.
- [23] Stanisław Jastrzębski, Zachary Kenton, Devansh Arpit, Nicolas Ballas, Asja Fischer, Yoshua Bengio, and Amos Storkey. Three factors influencing minima in sgd. *arXiv preprint arXiv:1711.04623*, 2017.
- [24] Christopher J Shallue, Jaehoon Lee, Joe Antognini, Jascha Sohl-Dickstein, Roy Frostig, and George E Dahl. Measuring the effects of data parallelism on neural network training. *arXiv preprint arXiv:1811.03600*, 2018.
- [25] Sam McCandlish, Jared Kaplan, Dario Amodei, and OpenAI Dota Team. An empirical model of large-batch training. *arXiv preprint arXiv:1812.06162*, 2018.
- [26] Guodong Zhang, Lala Li, Zachary Nado, James Martens, Sushant Sachdeva, George E Dahl, Christopher J Shallue, and Roger Grosse. Which algorithmic choices matter at which batch sizes? insights from a noisy quadratic model. *arXiv preprint arXiv:1907.04164*, 2019.
- [27] Stephan Mandt, Matthew D Hoffman, and David M Blei. Stochastic gradient descent as approximate bayesian inference. *The Journal of Machine Learning Research*, 18(1):4873–4907, 2017.
- [28] Samuel L Smith and Quoc V Le. A bayesian perspective on generalization and stochastic gradient descent. *arXiv preprint arXiv:1710.06451*, 2017.
- [29] Siyuan Ma, Raef Bassily, and Mikhail Belkin. The power of interpolation: Understanding the effectiveness of sgd in modern over-parametrized learning. *arXiv preprint arXiv:1712.06559*, 2017.
- [30] Elad Hoffer, Itay Hubara, and Daniel Soudry. Train longer, generalize better: closing the generalization gap in large batch training of neural networks. In *Advances in Neural Information Processing Systems*, pages 1731–1741, 2017.
- [31] Ping Luo, Xinjiang Wang, Wenqi Shao, and Zhanglin Peng. Towards understanding regularization in batch normalization. In *International Conference on Learning Representations*, 2019.
- [32] Nitish Srivastava, Geoffrey Hinton, Alex Krizhevsky, Ilya Sutskever, and Ruslan Salakhutdinov. Dropout: a simple way to prevent neural networks from overfitting. *The journal of machine learning research*, 15(1):1929–1958, 2014.
- [33] Kaiming He, Xiangyu Zhang, Shaoqing Ren, and Jian Sun. Deep residual networks github page: <https://github.com/kaiminghe/deep-residual-networks>, 2016.
- [34] Dmitry Ulyanov, Andrea Vedaldi, and Victor Lempitsky. Instance normalization: The missing ingredient for fast stylization. *arXiv preprint arXiv:1607.08022*, 2016.

- [35] Tim Salimans and Durk P Kingma. Weight normalization: A simple reparameterization to accelerate training of deep neural networks. In *Advances in Neural Information Processing Systems*, pages 901–909, 2016.
- [36] Yuxin Wu and Kaiming He. Group normalization. In *Proceedings of the European Conference on Computer Vision (ECCV)*, pages 3–19, 2018.
- [37] Andrew M Saxe, James L McClelland, and Surya Ganguli. Exact solutions to the nonlinear dynamics of learning in deep linear neural networks. *arXiv preprint arXiv:1312.6120*, 2013.
- [38] Devansh Arpit, Víctor Campos, and Yoshua Bengio. How to initialize your network? robust initialization for weightnorm & resnets. In *Advances in Neural Information Processing Systems*, pages 10900–10909, 2019.
- [39] Huishuai Zhang, Da Yu, Mingyang Yi, Wei Chen, and Tie-Yan Liu. Convergence theory of learning over-parameterized resnet: A full characterization, 2019.
- [40] Zeyuan Allen-Zhu, Yuanzhi Li, and Zhao Song. A convergence theory for deep learning via over-parameterization, 2018.
- [41] Simon S. Du, Jason D. Lee, Haochuan Li, Liwei Wang, and Xiyu Zhai. Gradient descent finds global minima of deep neural networks, 2018.
- [42] Yann A LeCun, Léon Bottou, Genevieve B Orr, and Klaus-Robert Müller. Efficient backprop. In *Neural networks: Tricks of the trade*, pages 9–48. Springer, 2012.

A Definition of a batch normalization layer

When applying batch normalization to convolutional layers, the inputs and outputs of normalization layers are 4-dimensional tensors, which we denote by $I_{b,x,y,c}$ and $O_{b,x,y,c}$. Here b denotes the batch dimension, c denotes the channels, and x and y are the two spatial dimensions. Batch normalization [4] applies the same normalization to every input in the same channel, such that:

$$O_{b,x,y,c} = \gamma_c \frac{I_{b,x,y,c} - \mu_c}{\sqrt{\sigma_c^2 + \epsilon}} + \beta_c.$$

Here, $\mu_c = \frac{1}{Z} \sum_{b,x,y} I_{b,x,y,c}$ denotes the per-channel mean, and $\sigma_c^2 = \frac{1}{Z} \sum_{b,x,y} I_{b,x,y,c}^2 - \mu_c^2$ denotes the per-channel variance, and Z is the normalization constant summed over the minibatch b and spatial dimensions x and y . A small constant ϵ is included in the denominator for numerical stability. The “scale” and “shift” parameters, γ_c and β_c , are learned during training. Typically, γ_c is initialized to 1 and β_c is initialized to 0, which is also what we consider in our analysis. Running averages of μ_c and σ_c^2 are also maintained during training, and these averages are used at test time to ensure the predictions are independent of other examples in the batch. For distributed training, the batch statistics are usually estimated locally on a subset of the training minibatch (“ghost batch normalization” [30]).

B Details of the residual networks used for figure 2

In figure 2 of the main text, we studied the variance of hidden activations and the batch statistics of residual blocks at a range of depths in three different architectures; a deep linear fully connected unnormalized residual network, a deep linear fully connected normalized residual network and a deep convolutional normalized residual network with ReLUs. We now define the three models in full.

Deep fully connected linear residual network without normalization: The inputs are 100 dimensional vectors composed of independent random samples from the unit normal distribution, and the batch size is 1000. These inputs first pass through a single fully connected linear layer of width 1000. We then apply a series of residual blocks. Each block contains an identity skip path, and a residual branch composed of a fully connected linear layer of width 1000. All linear layers are initialized with LeCun normal initialization [42] to preserve the variance in the absence of non-linearities.

Deep fully connected linear residual network with batch normalization: The inputs are 100 dimensional vectors composed of independent random samples from the unit normal distribution, and the batch size is 1000. These inputs first pass through a batch normalization layer and a single fully connected linear layer of width 1000. We then apply a series of residual blocks. Each block contains an identity skip path, and a residual branch composed of a batch normalization layer and a fully connected linear layer of width 1000. All linear layers are initialized with LeCun normal initialization [42] to preserve the variance in the absence of non-linearities.

Deep convolutional ReLU residual network: The inputs are batches of 100 images from the CIFAR-10 training set. We first apply a convolution of width 100 and stride 2, followed by a batch normalization layer, a ReLU non-linearity, and an additional convolution of width 100 and stride 2. We then apply a series of residual blocks. Each block contains an identity skip path, and a residual branch composed of a batch normalization layer, a ReLU non-linearity, and a convolution of width 100 and stride 1. All convolutions are initialized with He initialization [19].

In all three networks, we evaluate the variance at initialization on the skip path and at the end of the residual branch (we measure the empirical variance across multiple channels and multiple examples but for a single set of weights). For the two normalized networks, we also evaluate the mean moving variance and mean squared moving mean of the batch normalization layer (i.e., the mean value of the moving variance parameter and the mean value of the square of the moving mean, averaged over channels for a single set of weights). To obtain the batch normalization statistics, we set the momentum parameter of the batch normalization layers to 0, and then update the batch statistics once.

C The influence of ReLU non-linearities on batch normalization statistics

In the main text, we found that for the deep linear normalized residual network (figure 2(b)), the variance on the skip path is equal to the mean moving variance of the batch normalization layer, while

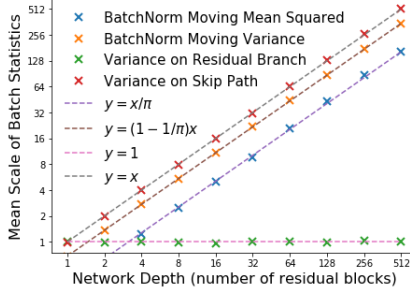


Figure 5: The batch statistics at initialization of a normalized deep fully connected network with ReLU non-linearities, evaluated on random inputs drawn from a Gaussian distribution.

the mean squared moving mean of the batch normalization layer is close to zero. However when we introduce ReLU non-linearities in the deep normalized convolutional residual network (figure 2(c)), the mean moving variance of the batch normalization layer is smaller than the variance across channels on the skip path, and the mean squared moving mean of the normalization layer grows proportional to the depth. To clarify the origin of this effect, we consider an additional fully connected deep normalized residual network with ReLU non-linearities. We form this network from the fully connected normalized linear residual network in appendix B by inserting a ReLU non-linearity after each normalization layer, and we replace LeCun initialization with He initialization. This network is easier to analyze than the convolutional network, but similar conclusions hold in both cases.

We provide the variance of the hidden activations and the batch statistics of this network in figure 5. The variance on the skip path in this network is approximately equal to the depth of the residual block d , while the variance at the end of the residual branch is approximately 1. This matches exactly our theoretical predictions in section 2 of the main text. Notice however that the mean moving variance of the batch normalization layer is approximately equal to $d(1 - 1/\pi)$, while the mean squared moving mean of the normalization layer is approximately equal to d/π . To understand these observations, we note that the outputs of a ReLU non-linearity have non-zero mean, and therefore the ReLU layer will cause the hidden activations of different examples on the same channel to become correlated (if the weights are fixed). Because of this, the variance across multiple examples and multiple channels becomes different from the variance across multiple examples for a single fixed channel.

To better understand this, we analyze this fully connected normalized ReLU residual network below. The input $X^0 \in \mathbb{R}^{w \times b}$ is a batch of b samples of dimension w that is sampled from a Gaussian distribution with mean $\mathbf{E}(X_{ij}^0) = 0$ and covariance $\mathbf{Cov}(X_{ik}^0, X_{jl}^0) = \delta_{ij}\delta_{kl}$, where δ_{ij} is the dirac delta function. The first dimension corresponds to the features and the second dimension corresponds to the batch. Let $W^0 \in \mathbb{R}^{w \times w}$ denote the linear layer before the first residual block, and for $\ell > 0$, let W^ℓ denote the linear layer on the residual branch of the ℓ -th residual block (we assume that all layers have the same width w for clarity in presentation). For each weight matrix W^ℓ , we assume that the elements of W^ℓ are independently sampled from $\mathcal{N}(0, 2/w)$ (He initialization). Let $X^\ell \in \mathbb{R}^{w \times b}$ denote the input to the ℓ -th residual block, let $X^+ = \max(X, 0)$ denote the ReLU non-linearity applied component-wise, and let \mathcal{B} denote the batch normalization operation. Thus, the input to the first residual block is given by $X^1 = W^0 \mathcal{B}(X^0)^+$, and the output of the ℓ -th residual block is given by $X^{\ell+1} = X^\ell + W^\ell \mathcal{B}(X^\ell)^+$ for $\ell > 0$. We want to analyze the batch normalization statistics for each layer. To this end, we begin by considering the input to the first residual block X^1 . Note that $X_{ij}^1 = \sum_k W_{ik}^0 \mathcal{B}(X^0)_{kj}^+$. The mean activation $\mathbf{E}(X_{ij}^1) = 0$, while the covariance,

$$\begin{aligned} \mathbf{Cov}(X_{ij}^1, X_{lm}^1) &= \mathbf{E} \left(\sum_{kn} W_{ik}^0 \mathcal{B}(X^0)_{kj}^+ W_{ln}^0 \mathcal{B}(X^0)_{nm}^+ \right) = \frac{2}{w} \delta_{il} \sum_k \mathbf{E} \left(\mathcal{B}(X^0)_{kj}^+ \mathcal{B}(X^0)_{km}^+ \right) \\ &\approx \delta_{il} \left(\frac{1 + (\pi - 1)\delta_{jm}}{\pi} \right). \end{aligned} \quad (1)$$

Since the components of X^0 are independent and Gaussian distributed, we have assumed that the components of $\mathcal{B}(X^0)$ are also independent and Gaussian distributed with mean $\mathbf{E}(\mathcal{B}(X^0)_{kj}) = 0$ and $\mathbf{Var}(\mathcal{B}(X^0)_{kj}) = 1$. This approximation is tight when the batch size is large ($b \gg 1$). It implies that $\mathbf{E}((\mathcal{B}(X^0)_{kj})^2) \approx 1/2$, and $\mathbf{E}(\mathcal{B}(X^0)_{kj}^+) \approx \sqrt{1/2\pi}$, from which we arrive at the equation 1.

We now consider the input to the second residual block $X^2 = X^1 + W^1 \mathcal{B}(X^1)^+$. To considerably simplify the analysis, we assume that the width w is large ($w \gg 1$). This implies that X^1 is Gaussian distributed with the covariance derived in equation 1 (See [13] for details). Once again, this implies that if the batch size b is also large then the components of $\mathcal{B}(X^1)$ are independent and Gaussian distributed with mean $\mathbf{E}(\mathcal{B}(X^1)_{ij}) = 0$ and $\mathbf{Var}(\mathcal{B}(X^1)_{ij}) = 1$ (note that batch normalization will remove the correlations between different examples in the batch in equation 1). This implies,

$$\mathbf{Cov}((W^1 \mathcal{B}(X^1)^+)_{ij}, (W^1 \mathcal{B}(X^1)^+)_{lm}) \approx \delta_{il} \left(\frac{1 + (\pi - 1)\delta_{jm}}{\pi} \right).$$

Furthermore, note that the covariance between the output of the residual branch and the skip connection, $\mathbf{Cov}((W^1 \mathcal{B}(X^1)^+)_{ij}, X_{lm}^1) = 0$. We therefore conclude that,

$$\begin{aligned} \mathbf{Cov}(X_{ij}^2, X_{lm}^2) &= \mathbf{Cov}(X_{ij}^1, X_{lm}^1) + \mathbf{Cov}((W^1 \mathcal{B}(X^1)^+)_{ij}, (W^1 \mathcal{B}(X^1)^+)_{lm}) \\ &\approx 2\delta_{il} \left(\frac{1 + (\pi - 1)\delta_{jm}}{\pi} \right). \end{aligned}$$

By induction, we can now see that the components of $\mathcal{B}(X^\ell)$ are independent and Gaussian distributed for all ℓ , and $\mathbf{Cov}((W^\ell \mathcal{B}(X^\ell)^+)_{ij}, X_{lm}^\ell) = 0$ for all ℓ . Thus, we get,

$$\mathbf{Cov}(X_{ij}^\ell, X_{lm}^\ell) \approx \ell \delta_{il} \left(\frac{1 + (\pi - 1)\delta_{jm}}{\pi} \right).$$

We are now ready to compute the expected values of the batch statistics, which we denote by μ^ℓ and σ^ℓ (see appendix A). The expected mean squared activation for a batch of examples on a single channel (the expected squared BatchNorm moving mean),

$$\mathbf{E}((\mu_c^\ell)^2) = \mathbf{E}\left(\left(\frac{1}{b} \sum_j X_{cj}^\ell\right)^2\right) = \frac{1}{b^2} \sum_{jk} \mathbf{E}(X_{cj}^\ell X_{ck}^\ell) \approx \ell \left(\frac{1}{\pi} + \frac{\pi - 1}{\pi b}\right) \approx \ell/\pi.$$

Meanwhile the expected variance across a batch of examples on a single channel (the expected BatchNorm moving variance),

$$\begin{aligned} \mathbf{E}((\sigma_c^\ell)^2) &= \mathbf{E}\left(\frac{1}{b} \sum_j (X_{cj}^\ell)^2 - \left(\frac{1}{b} \sum_j X_{cj}^\ell\right)^2\right) \\ &= \mathbf{E}\left(\frac{1}{b} \sum_j X_{cj}^\ell X_{cj}^\ell\right) - \mathbf{E}((\mu_c^\ell)^2) \approx \ell(1 - 1/\pi). \end{aligned}$$

These predictions exactly match our observations in figure 5. Our analysis shows how ReLU nonlinearities introduce correlations in the hidden activations between training examples (for shared random weights). These correlations cause the moving variance of the batch normalization layer, which is evaluated on a single channel for a single set of weights, to differ from the variance of the hidden activations over multiple random initializations (which we derived in section 2.1).

D Additional results on CIFAR-10

In table 3, we provide the minimum training losses, as well as the optimal learning rates at which the training loss is minimized, when training an n -2 Wide-ResNet for a range of depths n on CIFAR-10. At each depth, we train for 200 epochs following the training procedure described in section 2.3 of the main text. These results correspond to the same architectures considered in table 1, where we provided the associated test set accuracies. We provide the training loss excluding the L2 regularization term (i.e., the training set cross entropy), since one cannot meaningfully compare the L2 regularization penalty of normalized and unnormalized networks. These results confirm that batch normalization and SkipInit achieve similar training losses after the same number of training epochs.

Meanwhile, in figure 6 we provide the optimal learning rates of SkipInit, Regularized SkipInit and Batch Normalization, when training a 16-4 Wide-ResNet on CIFAR-10. These optimal learning rates correspond to the training losses and test accuracies provided in figure 4 of the main text. The batch statistics for batch normalization layers are evaluated over the full training minibatch.

Table 3: The training losses, and associated optimal learning rates, of an n -2 Wide-ResNet at a range of depths n . We train on CIFAR-10 for 200 epochs with either batch normalization or SkipInit.

Batch Normalization			SkipInit ($\alpha = 1$)		
Depth	Training loss	Learning rate	Depth	Training loss	Learning rate
16	0.007 ± 0.000	2^{-2} (2^{-2} to 2^{-2})	16	0.004 ± 0.000	2^{-3} (2^{-4} to 2^{-3})
100	0.001 ± 0.000	2^{-3} (2^{-3} to 2^{-2})	100	—	—
1000	0.001 ± 0.000	2^{-3} (2^{-4} to 2^{-3})	1000	—	—
SkipInit ($\alpha = 1/\sqrt{d}$)			Divide residual block by $\sqrt{2}$		
Depth	Training loss	Learning rate	Depth	Training loss	Learning rate
16	0.004 ± 0.000	2^{-3} (2^{-3} to 2^{-3})	16	0.013 ± 0.000	2^{-3} (2^{-3} to 2^{-3})
100	0.001 ± 0.000	2^{-4} (2^{-4} to 2^{-4})	100	0.066 ± 0.015	2^{-6} (2^{-6} to 2^{-6})
1000	0.001 ± 0.000	2^{-3} (2^{-4} to 2^{-3})	1000	—	—
SkipInit ($\alpha = 0$)			SkipInit without L2 ($\alpha = 0$)		
Depth	Training loss	Learning rate	Depth	Training loss	Learning rate
16	0.004 ± 0.000	2^{-3} (2^{-3} to 2^{-3})	16	0.008 ± 0.000	2^{-3} (2^{-3} to 2^{-3})
100	0.001 ± 0.000	2^{-4} (2^{-4} to 2^{-3})	100	0.001 ± 0.000	2^{-3} (2^{-4} to 2^{-2})
1000	0.001 ± 0.000	2^{-4} (2^{-4} to 2^{-4})	1000	0.000 ± 0.000	2^{-2} (2^{-2} to 2^{-2})

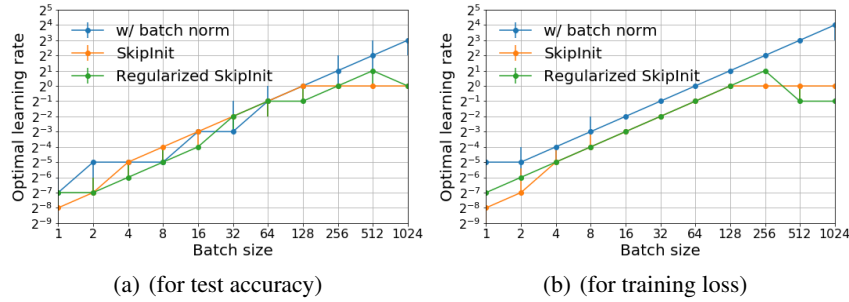


Figure 6: The optimal learning rates of SkipInit, Regularized SkipInit and Batch Normalization, for a 16-4 Wide-ResNet trained for 200 epochs on CIFAR-10. We evaluate the batch statistics over the full training minibatch. All three methods have similar optimal learning rates in the small batch limit.

E Additional results on CIFAR-100

In tables 4 and 5, we provide the optimal test accuracies and optimal training losses, and the corresponding optimal learning rates, when training n -2 WideResNets on CIFAR-100 for different depths n for 200 epochs. We follow the training protocol described in section 2.3 of the main text. Both batch normalization and SkipInit are able to train very deep Wide-ResNets on CIFAR-100.

In figure 7, we compare the performance of SkipInit, Regularized SkipInit (drop probability 0.6), and batch normalization across a wide range of batch sizes, when training a 28-10 Wide-ResNet on CIFAR-100 for 200 epochs. We follow the training protocol described in section 3 of the main text, but we use a ghost batch size of 32. We were not able to train the 28-10 Wide-ResNet to competitive performance when not using either batch normalization or SkipInit. Batch normalized networks achieve higher test accuracies at all batch sizes. However in the small batch limit, the optimal learning rate is proportional to the batch size, and the optimal learning rates of all three methods are approximately equal. As we observed in the main text, batch normalization has a larger maximum stable learning rate, and this allows us to scale training to larger batch sizes.

Finally, in figure 8, we repeat this comparison of SkipInit, Regularized SkipInit and batch normalization at a range of batch sizes, but instead of selecting a fixed ghost batch size, we evaluate the batch statistics of batch normalization layers across the full minibatch (as in section 4). We observe a clear regularization effect, whereby the test accuracy achieved with batch normalization peaks for a batch size of 16 and decays rapidly if the batch size is increased or decreased. Regularized SkipInit achieves higher test accuracies than normalized networks when the batch size is small, and it is also

Table 4: The optimal test accuracies and corresponding learning rates (with error bars), when training width 2 Wide-ResNets on CIFAR-100 for a wide range of depths. Both batch normalization and SkipInit are able to train very deep residual networks. However it is not possible to train depth 1000 networks if we do not downscale the hidden activations on the residual branch at initialization.

Batch Normalization			SkipInit ($\alpha = 1$)		
Depth	Test Accuracy (%)	Learning rate	Depth	Test Accuracy (%)	Learning rate
16	72.6 \pm 0.3	2^0 (2^{-1} to 2^0)	16	65.6 \pm 0.4	2^{-4} (2^{-4} to 2^{-4})
100	77.2 \pm 0.2	2^0 (2^{-1} to 2^0)	100	-	-
1000	78.0 \pm 0.1	2^0 (2^0 to 2^0)	1000	-	-
SkipInit ($\alpha = 1/\sqrt{d}$)			Divide residual block by $\sqrt{2}$		
Depth	Test Accuracy (%)	Learning rate	Depth	Test Accuracy (%)	Learning rate
16	69.3 \pm 0.2	2^{-1} (2^{-2} to 2^{-1})	16	69.3 \pm 0.2	2^{-2} (2^{-2} to 2^{-1})
100	74.2 \pm 0.1	2^{-1} (2^{-1} to 2^{-1})	100	60.2 \pm 1.0	2^{-5} (2^{-5} to 2^{-5})
1000	74.7 \pm 0.3	2^{-1} (2^{-1} to 2^{-1})	1000	-	-
SkipInit ($\alpha = 0$)			SkipInit without L2 ($\alpha = 0$)		
Depth	Test Accuracy (%)	Learning rate	Depth	Test Accuracy (%)	Learning rate
16	69.3 \pm 0.2	2^{-1} (2^{-2} to 2^{-1})	16	63.5 \pm 0.3	2^{-3} (2^{-3} to 2^{-3})
100	74.3 \pm 0.3	2^{-1} (2^{-1} to 2^{-1})	100	66.0 \pm 0.4	2^{-3} (2^{-3} to 2^{-3})
1000	74.7 \pm 0.3	2^{-1} (2^{-1} to 2^{-1})	1000	67.9 \pm 0.3	2^{-2} (2^{-2} to 2^{-2})

Table 5: The optimal training losses and corresponding learning rates (with error bars), when training width 2 Wide-ResNets on CIFAR-100 for a wide range of depths. Both batch normalization and SkipInit are able to train very deep residual networks. We show it is not possible to train depth 1000 networks if we do not downscale the hidden activations on the residual branch at initialization.

Batch Normalization			SkipInit ($\alpha = 1$)		
Depth	Training loss	Learning rate	Depth	Training loss	Learning rate
16	0.078 \pm 0.002	2^{-2} (2^{-2} to 2^{-2})	16	0.089 \pm 0.022	2^{-4} (2^{-5} to 2^{-4})
100	0.002 \pm 0.000	2^{-2} (2^{-2} to 2^{-2})	100	-	-
1000	0.001 \pm 0.000	2^0 (2^0 to 2^0)	1000	-	-
SkipInit ($\alpha = 1/\sqrt{d}$)			Divide residual block by $\sqrt{2}$		
Depth	Training loss	Learning rate	Depth	Training loss	Learning rate
16	0.050 \pm 0.003	2^{-3} (2^{-3} to 2^{-3})	16	0.062 \pm 0.002	2^{-3} (2^{-3} to 2^{-3})
100	0.002 \pm 0.000	2^{-4} (2^{-4} to 2^{-2})	100	0.394 \pm 1.270	2^{-5} (2^{-8} to 2^{-5})
1000	0.001 \pm 0.000	2^{-4} (2^{-5} to 2^{-2})	1000	-	-
SkipInit ($\alpha = 0$)			SkipInit without L2 ($\alpha = 0$)		
Depth	Training loss	Learning rate	Depth	Training loss	Learning rate
16	0.052 \pm 0.007	2^{-3} (2^{-3} to 2^{-2})	16	0.122 \pm 0.014	2^{-3} (2^{-4} to 2^{-3})
100	0.002 \pm 0.000	2^{-4} (2^{-4} to 2^{-2})	100	0.004 \pm 0.000	2^{-3} (2^{-4} to 2^{-3})
1000	0.001 \pm 0.000	2^{-4} (2^{-5} to 2^{-3})	1000	0.002 \pm 0.000	2^{-3} (2^{-3} to 2^{-3})

competitive with batch normalized networks when the batch size is moderately large. These results emphasize the importance of tuning the ghost batch size in batch normalized networks.

F Additional results on ImageNet

In table 6, we present the performance of batch normalization, Fixup and Regularized SkipInit when training Resnet-50-V1 [2] on ImageNet for 90 epochs. Unlike ResNet-V2 and Wide-ResNets, this network does not have an identity skip path, because it introduces a ReLU at the end of the residual block after the skip connection and residual branch merge. We find that Fixup performs slightly worse than batch normalization when the batch size is small, but considerably worse than batch normalization when the batch size is large (similar to the results on ResNet-50-V2). However,

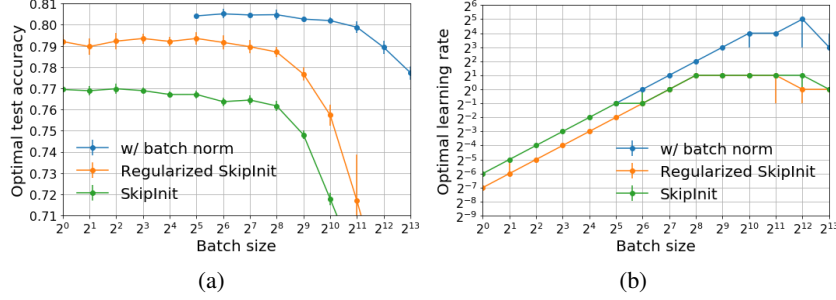


Figure 7: The optimal test accuracy, and the corresponding optimal learning rates of a 28-10 Wide-ResNet, trained on CIFAR-100 for 200 epochs. We were unable to train this network reliably without batch normalization or SkipInit (not shown). Batch normalized networks achieve higher test accuracies, and are also stable at larger learning rates, which enables large batch training.

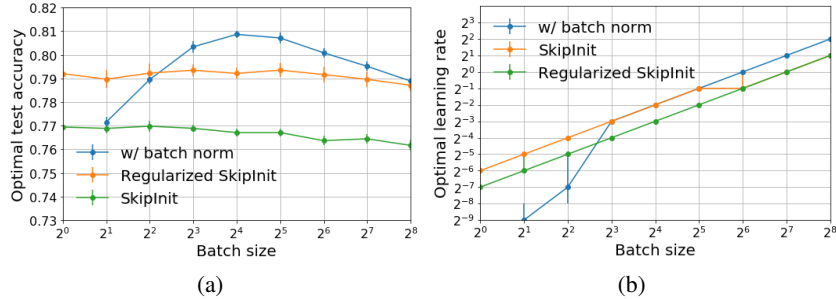


Figure 8: The optimal test accuracy, and the corresponding optimal learning rates of a 28-10 Wide-ResNet, trained on CIFAR-100 for 200 epochs. We do not use ghost batch normalization here, evaluating the batch statistics over the full minibatch. The test accuracy achieved with batch normalization depends strongly on the batch size, and is maximized for a batch size of 16. Regularized SkipInit achieves higher test accuracies than batch normalized networks when the batch size is very small, and it is competitive with batch normalized networks when the batch size is moderately large.

Regularized SkipInit is significantly worse than batch normalization and Fixup at all batch sizes. This is not surprising, since we designed SkipInit for models which contain an identity skip connection through the residual block. We also consider a modified version of Regularized SkipInit, which contains a single additional scalar bias in each residual block, just before the final ReLU (after the skip connection and residual branch merge). This scalar bias eliminates the gap in validation accuracy between Fixup and Regularized SkipInit when the batch size is small. We conclude that only two components of Fixup are essential to train the original ResNet-V1: initializing the residual branch at zero, and introducing a scalar bias after the skip connection and residual branch merge.

Table 6: We train ResNet50-V1 on ImageNet for 90 epochs. Fixup performs well when the batch size is small, but performs poorly when the batch size is large. Regularized SkipInit performs poorly at all batch sizes, but its performance improves considerably if we add a scalar bias before the final ReLU in each residual block (after the skip connection and residual branch merge). We perform a grid search to identify the optimal learning rate which maximizes the top-1 validation accuracy. We perform a single run at each learning rate and report both top-1 and top-5 accuracy scores. We use a drop probability of 0.2 for Regularized SkipInit. We note that ResNet-V1 does not have an identity skip connection, which explains why Regularized SkipInit performs poorly without scalar biases.

Test accuracy:	Batch size		
	256	1024	4096
Batch normalization	75.6 / 92.5	75.3 / 92.4	75.4 / 92.4
Fixup	74.4 / 91.6	74.4 / 91.7	72.4 / 90.3
Regularized SkipInit	70.0 / 89.2	68.4 / 87.8	68.2 / 87.9
Regularized SkipInit + Scalar Bias	75.2 / 92.4	74.9 / 92.0	70.8 / 89.6